Quantitative investigation of the pore size–reducing effect of perfluorocarbons in polyurethane foaming

Martin Hamann, Sébastien Andrieux, Markus Schütte, Daniel Telkemeyer, Meik Ranft, Wiebke Drenckhan-Andreatta

Colloid and Polymer Science
https://doi.org/10.1007/s00396-023-05107-z

ORIGINAL CONTRIBUTION

Quantitative investigation of the pore size–reducing effect of perfluorocarbons in polyurethane foaming

Martin Hamann[1] · Sébastien Andrieux[1] · Markus Schütte[2] · Daniel Telkemeyer[2] · Meik Ranft[3] · Wiebke Drenckhan[1]

Received: 6 February 2023 / Revised: 22 March 2023 / Accepted: 2 April 2023

Abstract

Despite the long-standing use of per- and polyfluorinated carbons (FCs) as pore size–reducing agents for polyurethane rigid (PUR) foams, their mechanisms of action remain poorly understood. To shed light on these mechanisms, we provide a quantitative analysis of the influence of the FC concentration on the pore size of PUR cup foams of two different model PUR foam systems: an industrially-relevant "technical system" and a simplified "scientific system." Combining scanning electron microscopy (SEM) and the PORE!SCAN method, we provide a detailed analysis of the pore size distributions of the obtained foams. We confirm that the characteristic pore size of both systems is indeed significantly reduced by adding small quantities of FC. However, we show that there seems to exist a critical FC concentration (about 3 wt.% with respect to the A-component) beyond which adding more FC has a negligible effect. More interestingly, the relative extent of the pore size reduction is almost identical for both PUR foam systems and the normalized pore size distributions remain largely unchanged over the whole range of FC concentrations. Our findings suggest that the FC-driven pore size reduction is a general effect caused by distinct mechanisms that are independent of the choice of the PUR foam system. Moreover, we hypothesize that this effect is not to be searched for during foam aging, as often reported, but during the pre-mixing step.

Keywords Polyurethane foam · Fluorocarbon · Morphology · Pore size distribution

Introduction

Polyurethane rigid (PUR) foams have been used in a wide range of applications since the 1960s with a focus on thermal insulation. However, the benchmark blowing agents for the preparation of PUR foams at the time were chlorofluorocarbons (CFCs) such as trichlorofluoromethane (also known as CFC-11). While the use of bromo- and chlorofluorocarbons as potent blowing agents and refrigerants flourished to reach its peak in the 1980s [1], they were identified [2, 3] to be the origin of the degeneration of the stratospheric ozone layer. As a consequence, governments, environmental organizations, and industrials teamed up to initiate a ban of bromo- and chlorofluorocarbons for the widespread use. The corresponding treaty ruling the use and the phaseout of CFCs is known as the Montreal Protocol [4] which was passed and applied in the late 1980s. Nearly 40 years later, it is delightful to mention that recent observations indeed indicate a continuous recovery of the stratospheric ozone layer in the last years [5, 6].

However, replacing CFCs adequately has been a major challenge for PUR foam producers ever since. Already in the 1990s, first studies proposed per- or polyfluorinated carbons, short, fluorocarbons (FCs), as promising candidates for next-generation (physical-)-blowing agents [7–10]. Similarly to CFC vapors, the low thermal conductivity of FC vapors renders them favorable pore-gases for thermally insulating PUR foams—materials that are currently highly sought-after in the context of rising energy prices and strict regulations on CO_2 emissions. In contrast to CFCs, however, FC molecules have the advantage of being very stable, such that the formation of ozone-depleting radicals in the stratosphere is avoided. Furthermore, Otto Volkert [7] demonstrated that small quantities of FCs in combination with

✉ Martin Hamann
martin.hamann@etu.unistra.fr

✉ Wiebke Drenckhan
wiebke.drenckhan@ics-cnrs.unistra.fr

[1] Institut Charles Sadron, CNRS-UPR 22, Université de Strasbourg, 67200 Strasbourg, France

[2] BASF Polyurethanes GmbH, 49448 Lemförde, Germany

[3] BASF SE, 67056 Ludwigshafen Am Rhein, Germany

Published online: 22 May 2023

other physical-blowing agents such as cyclopentane suffice to affect PUR foam morphology by significantly reducing the mean pore size. This FC-induced reduction of the mean foam pore size is particularly beneficial for the preparation of thermally insulating PUR foams, since it diminishes the contribution of thermal radiation to the overall thermal conductivity of a PUR foam [11, 12]. Thus, FCs may not only be considered as physical blowing agents but also as liquid-type pore size–reducing agents that give rise to potent thermally insulating PUR foams.

Unfortunately, FCs themselves are also associated with substantial environmental concerns. On the one hand, FCs exhibit significant global warming potential (GWP) [13, 14], i.e., they are very potent greenhouse gases. On the other hand, the molecular stability of FCs may give rise to an unwanted and persistent accumulation of these species in the atmosphere [15]. Thus, there is a growing interest in substituting FCs as pore size reducing agents by less critical alternatives. To achieve this, however, the origins of the FC-driven pore size reducing effect on PUR foam morphology need to be understood. Despite the fact that FCs have been used as pore size–reducing agents for decades, the understanding of the pore size–reducing effects has remained approximative, which is reflected by very different explanations being proposed in the preceding literature. Only recently, Brondi et al. [16] provided the first step to a more coherent scientific interpretation of the mechanisms responsible for the FC-driven pore size reduction. In short, their results demonstrate that the FCs strongly facilitates aeration, i.e., the mechanical entrainment of air bubbles into the system, while blending the reactive components forming the PUR foam and therefore favors the formation of smaller pores. This goes well in line with our own findings [17] that clearly show that there is indeed a reciprocal relation between the air bubble density in the initially liquid reactive mixture and the pore size of the final PUR foam. Additionally, Brondi et al. [16] suggest that the FC does not only facilitate the entrainment of air bubbles but also acts as an osmotic agent retarding Ostwald ripening during foam blowing, which is in line with a patent from Klostermann et al. [18].

The object of the study at hand is to advance our understanding of the underlying mechanisms responsible for the pore size reduction. For this purpose, we focus on studying quantitatively the impact of the FC concentration on the pore size distribution. To the best of our knowledge, such a systematic study has yet to be reported. We investigated the morphology of PUR foam batches prepared by mixing the two components of the formulation in small paper cups (so-called "cup foams") using two-component systems. The so-called "A-component" contained one or several polyols as well as blowing agents, a surfactant, catalysts, and the FC as a pore size–reducing agent, while the "B-component" consisted of an oligomeric form of methylene diphenyldiisocyanate (pMDI). We systematically varied the FC concentration within the A-component while keeping all other formulation parameters fixed, such that changes of the PUR foam morphology could be traced back exclusively to the variation of the FC concentration. We only adapted the concentration of the physical blowing agent (cyclopentane) with the FC concentration to maintain the final foam density constant for all formulations.

Furthermore, we focused on investigating whether the pore size reducing effect of the FC depends on the chosen polyols. For this purpose, the variation of the FC concentration was simultaneously performed for two different PUR foam model systems. For one of the two model systems, which we call "technical system," we chose a PUR foam formulation with the A-component containing a blend of three macromolecular polyether polyols. This system was chosen in order to mimic technically relevant PUR foam systems currently used by PUR foam manufacturers. In contrast to the technical system, we also used a second, simplified model system, which we refer to as the "scientific system" where the A-component contained only one low-molecular diol (tripropylene glycol (TPG)) as a polyol compound.

Materials, formulations, and methods

Materials

The macromolecular polyether polyols "Polyetherol 90060," "Polyetherol 90094," and "Polyetherol 90178" for the "technical system" were supplied by BASF. Tripropylene glycol (TPG; 97% by *Sigma-Aldrich*) was used as a low-molecular polyol for the "scientific system." For both formulations, the A-component contained a catalyst blend based on tertiary-amines provided by *BASF*. The silicone-based surfactant Tegostab B8491 (supplied by *Evonik Industries*) was used for both formulations. Water was used as a chemical blowing agent, while cyclopentane ($\geq$ 95%, *BASF*) and the fluorocarbon FA-188 (perfluoro(4-methylpent-2-ene); supplied by *3M*) were used as physical blowing agents. For all formulations, the B-component consisted of the isocyanate Lupranat M20S which was supplied by *BASF*. Lupranat M20S is an oligomeric form of methylene diphenyldiisocyanate with an NCO-content of ca. 31 wt.% and an average functionality of 3. All chemicals were used as received without prior purification.

Formulations

Two different model systems were chosen for the preparation of polyurethane rigid (PUR) foams. For both systems, the amount of the B-component was adapted to maintain

Table 1 Overview of the formulations used for PUR foam preparation

	Technical system								*Scientific system*							
Substance	**A-Component***															
Polyol blend [wt.%]	93.95	93.95	93.95	93.95	93.95	93.95	93.95	93.95	0	0	0	0	0	0	0	0
TPG [wt.%]	0	0	0	0	0	0	0	0	93.95	93.95	93.95	93.95	93.95	93.95	93.95	93.95
Surfactant [wt.%]	2.0	2.0	2.0	2.0	2.0	2.0	2.0	2.0	2.0	2.0	2.0	2.0	2.0	2.0	2.0	2.0
Catalyst [wt.%]	1.55	1.55	1.55	1.55	1.55	1.55	1.55	1.55	1.55	1.55	1.55	1.55	1.55	1.55	1.55	1.55
H_2O [wt.%]	2.5	2.5	2.5	2.5	2.5	2.5	2.5	2.5	2.5	2.5	2.5	2.5	2.5	2.5	2.5	2.5
	Physical blowing agents*															
Cyclopentane [wt.%]	13.5	13.3	13.0	12.8	12.6	12.3	12.1	11.2	13.5	13.3	13.0	12.8	12.6	12.3	12.1	11.2
FA-188 [wt.%]	0	1	2	3	4	5	6	10	0	1	2	3	4	5	6	10
	B-Component*															
Iso M20S [wt.%] ($I_{NCO}=120$)	136.7	136.7	136.7	136.7	136.7	136.7	136.7	136.7	197.8	197.8	197.8	197.8	197.8	197.8	197.8	197.8

* with respect to 100 wt.% of the A-component

a fixed isocyanate-index of $I_{NCO}=120$. Moreover, the amount of blowing agents (water, cyclopentane, and optionally perfluoro(4-methylpent-2-ene)) was the same for both systems to ensure that all obtained foams have a density of $\rho=(30\pm2)$ g L^{-1}. To maintain a constant density, the cyclopentane concentration was systematically adjusted with the FC concentration. Furthermore, the same surfactant concentration ($c_{surf}=2.00$ wt.%) and catalyst concentration ($c_{cat}=1.55$ wt.%) were applied for both systems. Note that both c_{surf} and c_{cat} correspond to concentrations typically used in industrial R&D labs for the preparation of PUR foams with good stability and reasonable reaction kinetics. Table 1 provides a detailed overview of all PUR foam formulations used throughout the study at hand. In total, the mass of the overall reactive PUR foam systems containing the A-component, the B-component, and the blowing agents ranged from ca. 50 to 55 g depending on the system and the formulation.

The major difference between the systems was the choice of the polyol(s) in the A-component. While for the "technical system," the A-component consisted of a blend of three macromolecular polyether polyols (Table 2), tripropylene glycol (TPG) was used as a single low-molecular polyol in the "scientific system." Table 1 lists all the individual constituents and their respective concentrations for all variations of both the technical system and the scientific system. A detailed description of how the formulations were prepared and mixed is provided in "Methods."

Methods

Preparation of PUR cup foams

For the technical system, a batch of the polyol blend was prepared roughly an hour before PUR foam generation via continuous, vigorous mixing of the individual polyols for at least 45 min. Then, the overall A-component was prepared by weighing the individual substances into a paper cup ($V=735$ ml) according to the formulations given in Table 1. Next, the physical-blowing agent(s) were added to the A-component and homogenized using a motorized overhead stirrer equipped with a *Lenart-Disc* geometry at a stirring speed of 1400 rpm for 15 ± 3 s. Then, the B-component was added rapidly followed immediately by intensive blending of both components at 1400 rpm for 5–7 s. Subsequent to blending, the generation of a PUR foam in the paper cup containing the liquid reactive mixture was triggered. For the

Table 2 Overview of the composition of the polyether polyol blend used for the "technical system" and the "scientific system," including the corresponding hydroxyl value HV and viscosities η

Substance	**Polyol blend [wt.%] (tech. sys. only)**	**Hydroxyl value HV [mgKOH/g]**	**Viscosity η [mPas] ($T=25$ °C)**
Technical system			
Polyetherol 90060	50	490	8450
Polyetherol 90094	10	160	300
Polyetherol 90178	40	390	12,800
		Weighted mean: 420	
Scientific system			
Tripropylene glycol (TPG)	100	570	78

technical system, the cream time was 11 ± 2 s while the gel time was 60 ± 2 s. In contrast, for the scientific system, the cream time was 17 ± 3 s and gel time 64 ± 2 s. Note that the given cream and gel times correspond to mean values with standard deviations of at least three repetitions of the PUR foam preparation. Moreover, the presence of the FC did not have a notable impact on neither the cream time nor the gel time irrespective of the chosen system. After cup foam formation was completed, the foams rested to cool down to room temperature. The full procedure was conducted at room temperature (20 °C) under a fume hood.

Measurement of the PUR foam density

Once PUR foam preparation was finished and the obtained PUR foam had cooled down to room temperature, the part of the risen PUR foam that exceeded the height of the paper cup was cut off to align the foam volume and the cup volume ($V = 735$ mL). Next, the mass of the PUR foam was weighed to determine the foam's density after removal of the weight of the paper cup.

Characterization of the PUR foam morphology via scanning electron microscopy (SEM)

For SEM analyses, cubic samples with an edge length of ~ 5 cm were cut from the center of the PUR foam using a band saw as is shown in Fig. 1a. Then, at least two thin slices of foam (thickness < 2 mm) were cut from each cubic foam sample using a razorblade (shaded square indicated in Fig. 1b). The different slices were taken from opposing corners of the upper face of the cube that was orientated perpendicularly to the direction of foam rise. The foam slices were fixed on a SEM sample holder with an adhesive carbon tape that allows for dissipation of electric charges. A *Hitachi SU 8010* SEM was used for all SEM investigations. For image acquisition, secondary electron detection was used together with an accelerating voltage of 1.0 kV and a beam current of 10 µA.

Statistical pore size analysis using the PORE!SCAN technique

The PORE!SCAN apparatus by Goldlücke GmbH (Fig. 2a) was used to automatically measure high numbers of pore sizes (several hundreds to thousands). For this purpose, a black carbon spray was applied on a plane cut of a PUR foam sample. The blackened sample was then placed inside the apparatus and micrographs were recorded iteratively from different angles of illumination via the circular arrangement of red diodes shown in Fig. 2a. Using the image processing and analysis tools of the PORE!SCAN unit, the individual micrographs were superimposed which results in a micrograph-stack (Fig. 2b) with a high contrast between the plateau borders, the pore struts (both bright), and the pore volume (black). This high contrast facilitates a clear binarization of the micrograph, which, in turn, enables automated pore detection and evaluation (Fig. 2c). Subsequently, the pore size data obtained from PORE!SCAN analysis was processed using the software Origin by OriginLabs to access the sample's pore radius distribution (Fig. 2d). Weibull distribution curves were fitted to the experimentally obtained pore radius distributions in order to describe the pore radius distribution numerically.

Results and discussion

Having prepared cup foams with different FC concentrations for both systems (technical and the scientific system), the obtained foams were first characterized using scanning electron microscopy (SEM) to visualize their porous morphology. A representative selection of images is shown in Fig. 3. Note that the PUR foam density was kept constant at $\rho = (30 \pm 2)$ g L^{-1} throughout the study to rule out misinterpretation of observations that could otherwise arise from changes in density.

As can be taken from Fig. 3, homogeneous macroporous morphologies were observed for all PUR cup foams

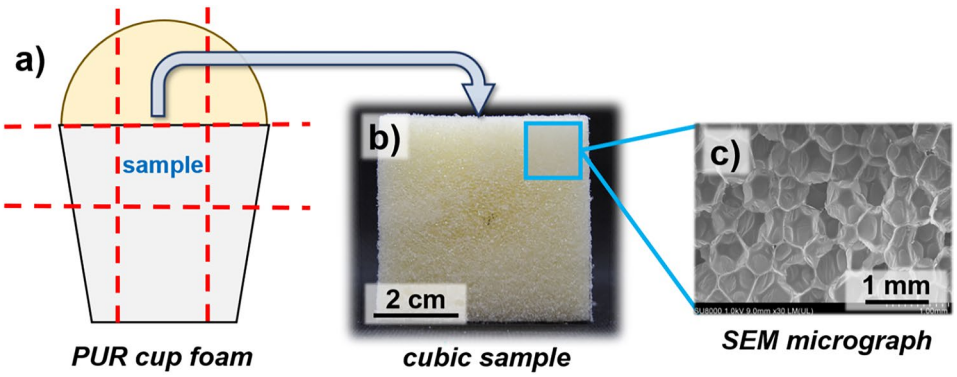

Fig. 1 **a**) Cuts (red-dashed lines) through the cup foams for the preparation of cubic PUR foam samples. **b**) Photograph of a cubic PUR foam sample obtained upon cutting of a cup foam. **c**) close-up image of the porous morphology of a cubic PUR foam sample acquired using scanning electron microscopy (SEM)

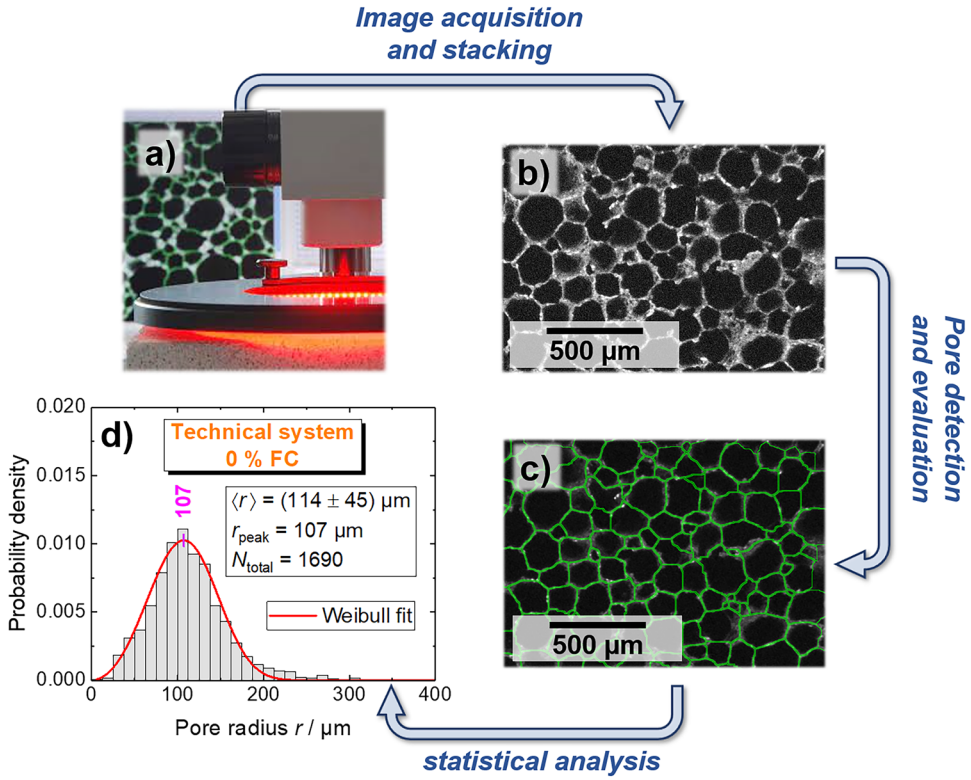

Fig. 2 Overview of the different steps involved in the characterization of porous PUR foam morphologies using the PORE!SCAN unit. **a**) Image of the PORE!SCAN apparatus by Goldlücke GmbH. **b**) Example of a micrograph obtained upon image acquisition from multiple angles of illumination and superposition of the individual images. **c**) Micrograph processed using the software for automated pore detection and evaluation provided by the PORE!SCAN unit. **d**) Pore radius distribution (gray histogram) obtained upon statistical analysis of the detected pore sizes as well as a Weibull distribution (red line) fitted to the histogram

with pore sizes ranging from several tens to a few hundred micrometers. One notices that foams prepared using the technical system (Fig. 3a) have smaller pores in general than those prepared with the scientific system (Fig. 3b). All SEM micrographs exhibit a predominantly closed pore foam morphology independent of both the chosen PUR foam system and the FC concentration. Furthermore, increasing the FC concentration does not seem to cause fundamental changes to the nature of the morphology (pore connectivity), except for the expected decrease of the average pore size.

To evaluate this FC-driven pore size reduction more quantitatively, full pore size statistics of the cup foam samples were prepared using the PORE!SCAN technique ("Methods"). These statistics were used to produce detailed pore radius distributions, examples of which are shown in Fig. 4. Empirically, we found that Weibull distributions [19] (red curves in Fig. 4) most accurately fitted the obtained histograms numerically for both systems and all FC concentrations. Note that an extended overview of all measured pore size distributions and the respective Weibull distribution fits is provided in the supporting information (SI Figs. S1 and S2). These distributions have also proven useful in the preceding literature for the description of both bubble size distribution in liquid aqueous foams [20, 21] as well as pore size distribution in PU foams [22]. One of the main reasons why Weibull distribution are well-suited for describing bubble/pore size distributions of many foam systems is that they take into account that the probability of bubble/pore extinction depends on an intricate coupling of the age and size of the bubbles/pores. Furthermore, these distributions allow to capture well the slight asymmetry of most of the obtained distributions. One needs to keep in mind that the presented distributions are obtained from 2D cuts of 3D foam samples. Therefore, the characteristic pore size of the 2D cut will appear smaller than the actual 3D pore size, since, statistically spoken, most pores are cut above or below the equator. In principle, one can account for this discrepancy by applying a geometrical correction factor [23, 24] of ~ 1.27 to the characteristic pore size irrespective of the pore polydispersity. Moreover, the 2D characterization of 3D pores also convolutes the actual pore size distribution with the distribution of where a pore is cut with respect to its equator [23]. Hence, even a perfectly monodisperse PUR foam would have a symmetric distribution around a peak corresponding to the pore size due to the chosen characterization approach. Unfortunately, disentangling these two distributions is not trivial and was therefore beyond of the scope of this study. As a consequence, we decided not to apply corrections to the pore size data obtained from PORE!SCAN analysis and work with the data as acquired. However, we emphasize that we are not primarily interested in obtaining precise absolute values but in investigating how both the characteristic pore size and the pore size distribution evolve with increasing FC concentrations. Thus, the chosen 2D characterization technique remains a reasonable approach despite the mentioned drawbacks.

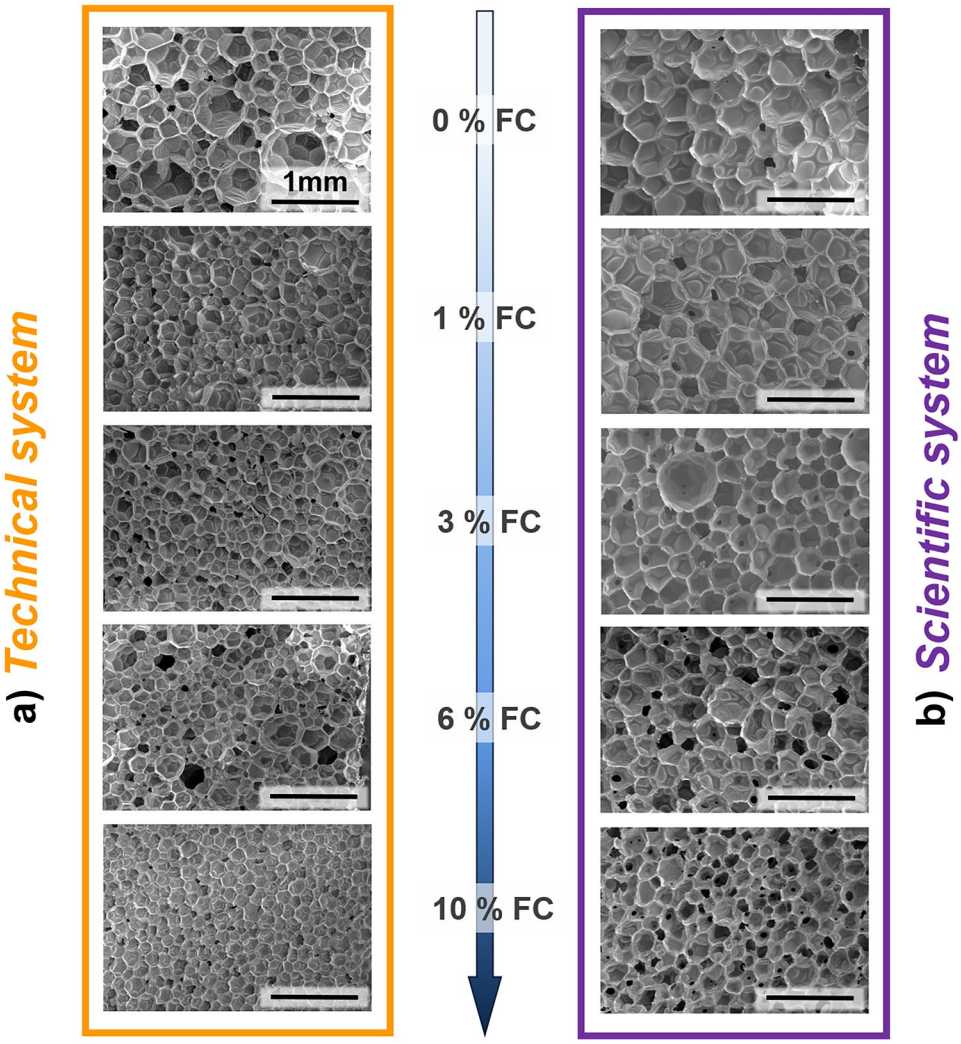

Fig. 3 SEM images of PUR cup foams prepared with different fluorocarbon concentrations for **a**) the technical system and **b**) the scientific system. Note that the FC concentrations correspond to mass concentrations with respect to 100 wt.% of the A-component

To understand how the FC concentration influences the pore size distribution of PUR foams, diagrams containing all the distributions from the technical and scientific systems with increasing FC concentrations are presented in Fig. 5. Note that for the sake of clarity, only the Weibull distribution curves fitted to the experimental data obtained upon PORE!SCAN analysis are shown in Fig. 5a and b. Moreover, note that an overview of all experimental pore size distributions obtained in the scope of this study as well as the respective Weibull distribution fits are provided in the supporting information (Figs. S1 and S2).

Figure 5a and b demonstrate that increasing the FC concentration leads to a shift of the pore size distributions towards smaller pores as was already suggested by the SEM micrographs shown in Fig. 3. While for the technical system the peak pore radii $\hat{r}_p$ of the distributions range from 110 µm for the FC-free sample to 70 µm at the highest FC concentration ($c = 10$ wt.% with respect to the A-component), the peak pore radii range from 180 µm (no FC) to 110 µm ($c = 10$ wt.% FC) for the scientific system. To highlight how the pore size evolves with the FC concentration, we plot the peak pore radius $\hat{r}_p$ as a function of FC concentration c in Fig. 6a. Note that we chose the peak pore radius $\hat{r}_p$ as a characteristic pore size instead of the arithmetic mean, since the obtained distributions are not necessarily symmetric such that the arithmetic mean may not always be very representative for the pore size distribution. The fact that foams prepared with the technical system exhibit smaller pores is most probably owed to the A-component of the technical system being ~ 85 times more viscous than that of the scientific system, since highly viscous systems are known to favor the formation of finer pores [25]. Figure 6a also demonstrates that the reduction of the peak pore radius $\hat{r}_p$ with increasing FC concentration c progresses very similarly for both systems. To be more precise, in both cases, a steady decrease of the peak pore radius $\hat{r}_p$ is observed up to an FC concentration of $c \approx 3$ wt.% before a plateau is reached. Further increasing the FC concentration does not seem to give rise to PUR foams with considerably smaller pores. Since both curves behave that remarkably similar, we normalized both curves shown in Fig. 6a using the peak pore radii $\hat{r}_{p,0}$ of the corresponding FC-free foams. The

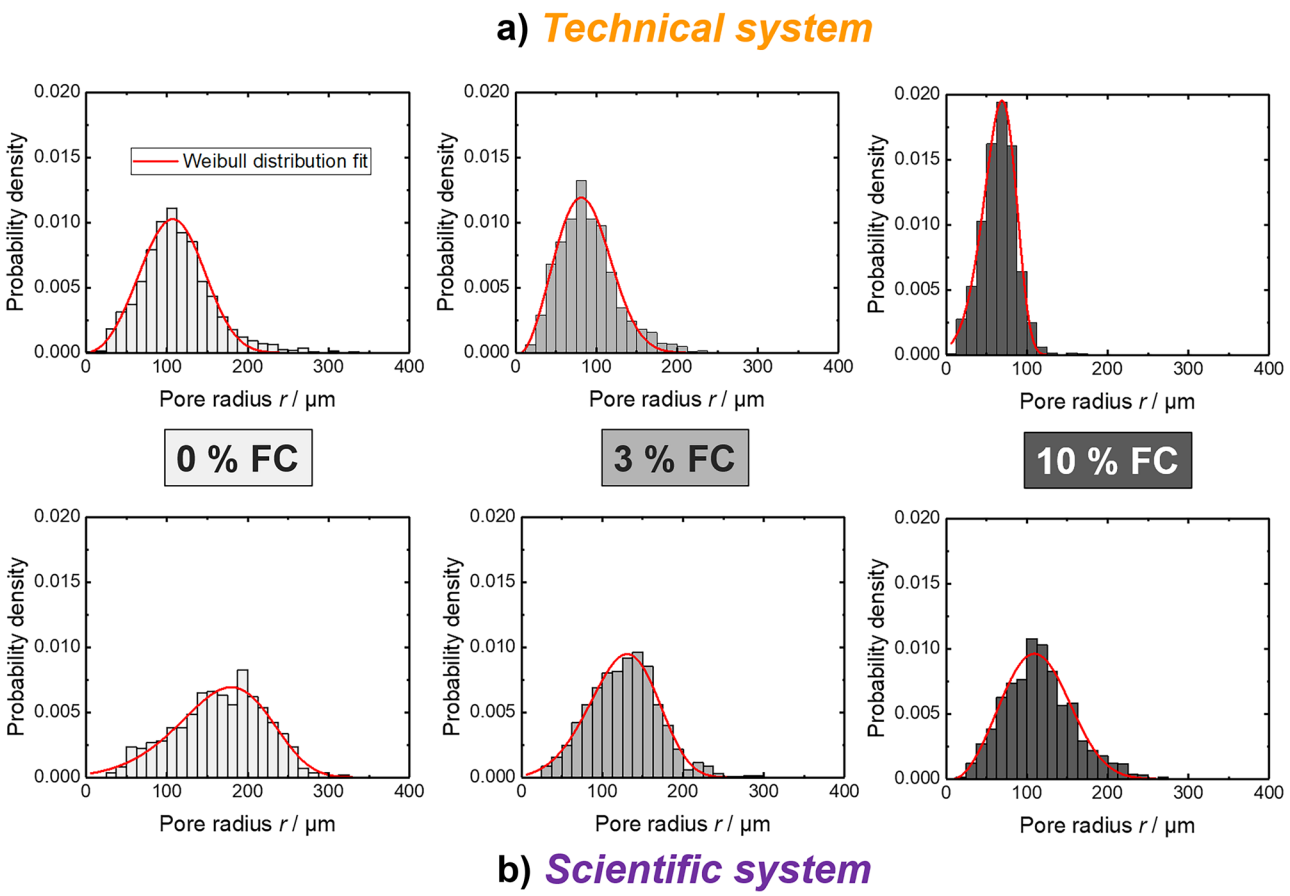

Fig. 4 Experimentally obtained pore size distributions (histograms) of PUR cup foams prepared with different FC concentration for both **a**) the technical system and **b**) the scientific system. The continuous red curves represent Weibull distributions fitted to the experimental data

resulting diagram is shown in Fig. 6b. In fact, both normalized curves clearly collapse onto one single master curve, which demonstrates that the relative extent of the pore size reduction with increasing FC concentration is actually the same for both systems. Interestingly, this finding suggests that the physicochemical mechanism(s) directing the FC-driven pore size could be independent of the PUR foam system. However, we emphasize that future studies need to confirm this hypothesis for a wider range of PUR foam formulations.

Lastly, we analyze how the overall shapes of the pore size distributions change with increasing FC concentration, as the shape of the distributions may give an indication of different aging phenomena [20, 26, 27] acting in the liquid foam state during PUR foam blowing. To efficiently compare the shapes of the different pore size distributions shown in Fig. 5a and b, we normalized all distributions by their respective peak pore radius $\hat{r}_p$. The normalized distribution obtained for the technical system are shown in Fig. 5c, while those obtained for the scientific system are shown in Fig. 5d.

Inspecting the normalized distribution of the technical system (Fig. 5c), we can capture that for low FC concentrations, the normalized distributions appear widened with respect to the FC-free reference while for FC concentrations higher than $c = 3$–4 wt.%, the normalized distributions are narrower than that of the FC-free reference. In contrast, the trend is basically inverse for the scientific system (Fig. 5d). Here, a certain tightening of the normalized distributions with respect to the FC-free reference foam can be registered for low FC concentrations of $c = 1$–2 wt.%, whereas the normalized distributions corresponding to higher FC concentrations are widened. Generally spoken, however, the changes of the normalized distributions are small, as all distributions are rather similar irrespective of the chosen PUR foam system or the FC concentration. This is also confirmed by plotting the normalized full width at half maximum (FWHM) which is shown as a function of the FC concentration c in Fig. 6c.

$$\varepsilon = \frac{\mathrm{FWHM}}{\hat{r}_\mathrm{p}}, \tag{1}$$

This factor ε can be understood as a measure for the pore polydispersity. As can be taken from Fig. 6, the resulting

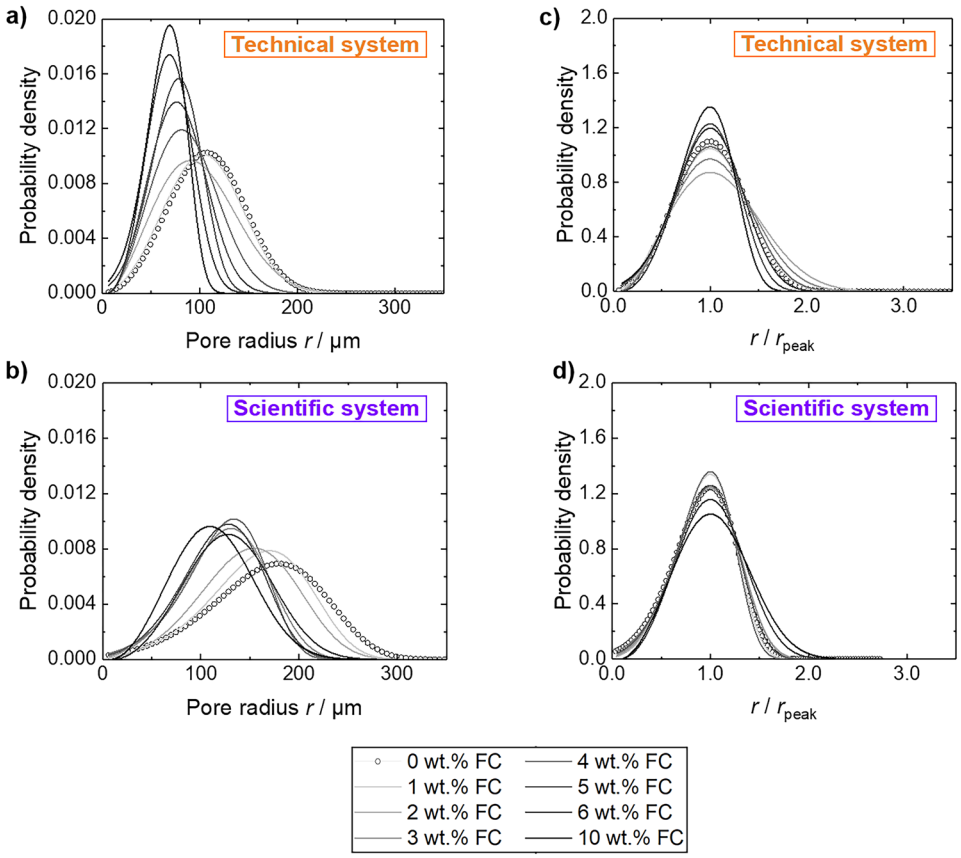

Fig. 5 Weibull distributions fitted to experimental pore size distributions obtained for PUR foams prepared with **a**) the technical system or **b**) the scientific system. Normalized pore radius distributions of the PUR foams prepared with either **c**) the technical system or **d**) the scientific system and different FC concentrations. All distributions were normalized using the respective peak pore radius as a normalization factor

values range between 0.7 and 1.2 for both PUR foam systems. Although they tend to slightly decrease with increasing FC concentration c for the technical system, while they slightly increase for the scientific system, a systematic impact of the FC concentration on the pore polydispersity cannot be recognized.

Since the impact of the different foam aging effects on the bubble size distribution of liquid foams is by now well understood [28, 29], we reason as follows: Although the FC may indeed interfere with foam aging phenomena during PUR foam blowing and solidification, we argue that this effect is only subtle and may not even always be in favor of the formation of smaller pores. Globally, two main aging phenomena that can occur are the coalescence of bubbles and gas exchange between bubbles (coarsening) [30]. The former is known to lead to the formation of much larger bubbles/pores via the rupture of films separating two neighboring bubbles/pores in close contact and would therefore be associated with the appearance of exceptionally large pores in the distributions [26, 31]. This is certainly not observed, which is why we can omit coalescence as relevant aging factor in all tested formulations, including those with high FC concentration. This is an important first conclusion, since the strongly hydrophobic FC droplets could easily serve as anti-foaming agents [32] at high concentrations. The latter aging phenomenon, coarsening, is more progressive. It typically leads to log-normal distributions with an asymmetry towards larger bubbles [33, 34]. The presence of FCs in the gas phase is known to inhibit coarsening in aqueous foams [35, 36] due to its insolubility in water and the associated osmotic pressure differences its vapor creates between bubbles. Much of the existing literature [16, 18] claims that an important part of the effect of FCs on the pore size reduction in PUR foams can be explained by the very same effect. However, the distributions of Fig. 5c and d do not support this hypothesis, since all distributions, irrespective of the FC concentration, are rather symmetric indicating that the PUR foams solidified quickly, leaving little time for coarsening to act. Moreover, as already mentioned, increasing the FC concentration does not necessarily tighten the distributions, which would be expected if the FC indeed reliably suppressed foam coarsening. One should also keep in mind that even at low FC concentrations, both the liquid and the gas phases of the foam are fully saturated with FC, making any osmotic argument implausible. Moreover, since the main foaming gases (CP and FC) are badly soluble in the liquid matrix, the characteristic time required for coarsening to have a measurable impact is much longer than the short-time window offered before solidification. In contrast, we claim that the FC-driven pore size reduction is predominantly due

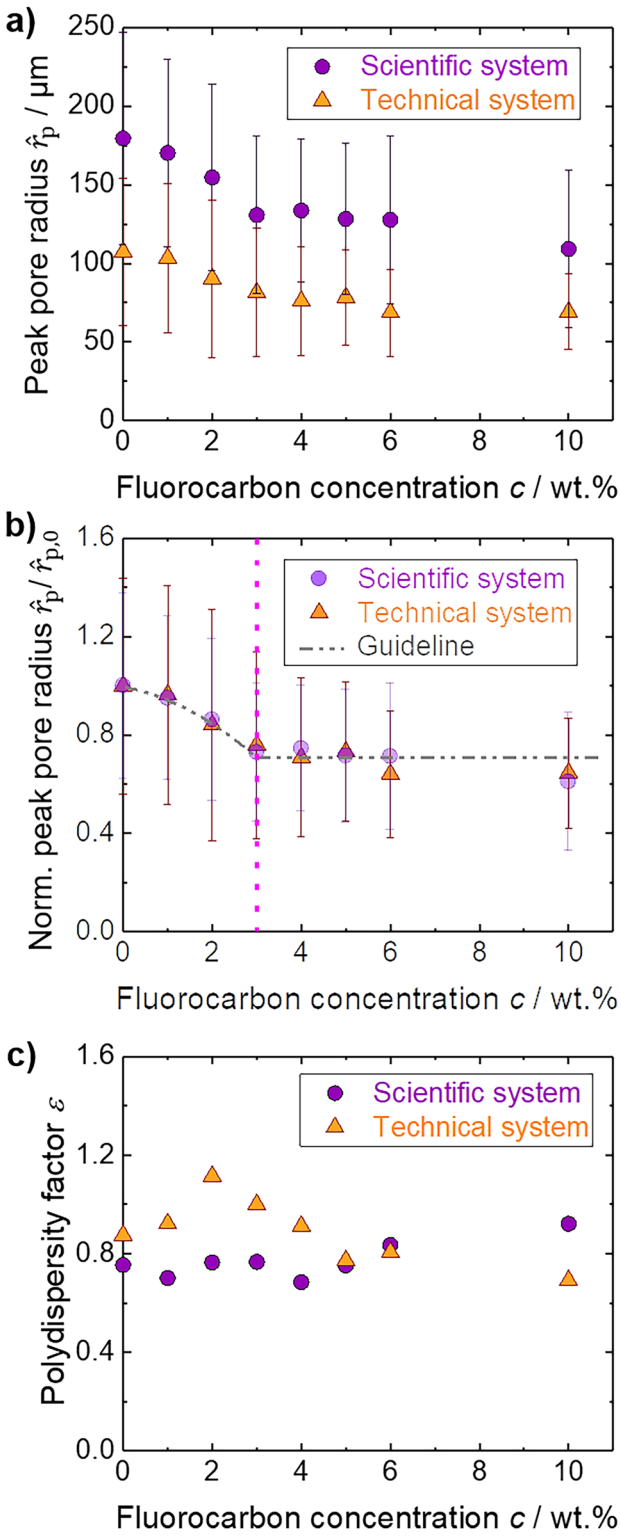

Fig. 6 **a**) Peak pore radii $\hat{r}_p$ of the distribution curves shown in Fig. 5a) and b) as a function of the FC concentration. The error bars correspond to the half width at half maximum (±HWHM) of the distributions. **b**) Peak pore radii $\hat{r}_p$ normalized by the peak pore radii $\hat{r}_{p,0}$ of the FC-free reference samples as a function of the FC concentration. **c**) Pore size polydispersity factors ε of the distributions shown in Fig. 5a) and b) as a function of the FC concentration

to the higher amounts of air bubbles being entrained into the system while blending the reactive components in the presence of FC, as was also recognized by Brondi et al. [16] and by ourselves [17]. In this context, we recently put in evidence a quantitative correlation between the characteristic pore size of PUR foams and the number of pre-dispersed air bubbles within the initially liquid reactive mixture. Furthermore, we will show in a follow-up study [35] (which goes beyond the scope of the paper at hand) that foams prepared without and with FCs obey the same correlation between air bubble density and foam pore size.

Summary and conclusion

In summary, we conducted a cup foam study to establish a quantitative correlation between the FC concentration used in PUR foam formulations and the resulting extent of the FC-driven pore size reduction. Furthermore, we investigated if the extent of this pore size reduction depends on the choice of the PUR foam system. For this purpose, we concepted a technically relevant PUR foam model system as well a simplified scientific model system. For both systems, PUR cup foams were prepared with different FC concentrations, whereas all other formulation parameters remained unchanged to highlight the impact of the FC on morphological changes of the obtained PUR foams. Scanning electron microscopy (SEM) revealed that for both systems macroporous PUR foams were obtained. However, the foams prepared with the technical system showed smaller pores in general, which is most probably due to the much higher viscosity of the technical system. Moreover, SEM analysis demonstrated that apart from a significant pore size reduction, increasing the FC concentration did not fundamentally affect the nature of the porous morphology.

Next, statistical analysis of the data obtained from the PORE!SCAN characterization complemented the observations made with SEM. While the characteristic pore radius decreased from 110 to 70 µm with increasing FC concentration for the technical system, characteristic pore radii between 180 and 110 µm were found for the scientific system depending on the FC concentration. More interestingly, the statistical analysis revealed that a limit of the pore size reducing effect is met at an FC concentration of $c \approx 3$ wt.%—for both systems. However, the most striking finding is that the relative extent of the pore size reduction is equivalent for both systems for all of the investigated FC concentrations, as shown by the master curve of Fig. 6a. This finding suggests that the FC-driven pore size reduction is very likely a general effect that is independent of the chosen PUR foam system and that there must be distinct mechanisms governing this effect. Future studies with

a wider range of PUR foam formulations are needed to unambiguously confirm this hypothesis.

Lastly, we compared the shapes of normalized pore radius distributions of PUR foams prepared with different systems and different FC concentrations to study a potential impact of the FC on aging phenomena during PUR foam blowing and solidification. We show that the peak pore size is the only morphological parameter significantly affected by the FC content, since the pore size distribution remains largely constant within the measurement errors. Moreover, the pore size distribution is fairly symmetrical, even in the absence of FC, suggesting that aging phenomena such as coalescence and diffusional coarsening are negligible during the foaming process and little affected by the presence of FC. This statement seems surprising in contrast to much of the previous literature [16, 18] that assumes the FC to act as a coarsening inhibitor, which is known from aqueous foams [35, 36]. However, we believe that the liquid matrix being saturated with FC droplets prohibits the creation of osmotic pressure gradients, which is required to suppress coarsening. Even though the FC droplets evaporate upon foam formation, the foam matrix is quickly too solid to allow for a significant impact of coarsening.

We therefore argue that the main impact of the FC on the pore size is not due to its impact on foam aging. In contrast, as recently shown and by Brondi et al. [16] and by our own work [17], we argue that the predominant pore size reducing effect of FCs is to facilitate the entrainment of air bubbles into the reactive PUR foam system which serve as precursors for the foam pores. This will be addressed systematically in upcoming studies.

Supplementary Information The online version contains supplementary material available at https://doi.org/10.1007/s00396-023-05107-z.

Acknowledgements The authors gratefully acknowledge the PLAMICS facility of the Institute Charles Sadron for providing access to the SEM. Moreover, the authors gratefully acknowledge the foam characterization department of BASF Polyurethanes GmbH for performing the experimental aspect of the PORE!SCAN analysis and for providing the data. We thank Aurélie Hourlier-Fargette, Leandro Jacomine, and Marie-Pierre Krafft for fruitful discussion.

Funding This work has been financed by BASF and an ERC Consolidator Grant (agreement 819511—METAFOAM). It also profited from an IdEx Unistra "Attractivity grant" (Chaire W. Drenckhan). Overall, it was conducted in the framework of the Interdisciplinary Institute HiFunMat, as part of the ITI 2021–2028 program of the University of Strasbourg, CNRS and Inserm, was supported by IdEx Unistra (ANR-10-IDEX-0002) and SFRI (STRATUS project, ANR-20-SFRI-0012) under the framework of the French Investments for the Future Program.

Data availability The data can be obtained contacting the corresponding author Wiebke Drenckhan under wiebke.drenckhan@icscnrs.unistra.fr.

Declarations

Conflict of interest The authors declare no competing interests.

References

1. European Environment Agency (2022) Consumption of ozone-depleting substances https://www.eea.europa.eu/ims/consumption-of-ozone-depleting-substances. Accessed 4 Oct 2022
2. Farman JC, Gardiner BG, Shanklin JD (1985) Large losses of total ozone in Antarctica. Nature 315:207–210. https://doi.org/10.1038/315207a0
3. Solomon S, Garcia RR, Rowland FS, Wuebbles DJ (1986) On the depletion of Antarctic ozone. Nature 321:755–758. https://doi.org/10.1038/321755a0
4. UN Environment Programme (2022) About Montreal Protocol https://www.unep.org/ozonaction/who-we-are/about-montreal-protocol. Accessed 9 Jun 2022
5. Solomon S, Ivy DJ, Kinnison D, Mills MJ, Neely III RR, Schmidt A (2016) Emergence of healing in the Antarctic ozone layer. Science (80-.) 353(6296):269–274. https://doi.org/10.1126/science.aae0061
6. Chipperfield MP, Bekki S, Dhomse S, Harris NRP, Hassler B, Hossaini R, Steinbrecht W, Thiéblemont R, Weber M (2017) Detecting recovery of the stratospheric ozone layer. Nature 549(7671):211–218. https://doi.org/10.1038/nature23681
7. Volkert O (1992) PUR Foams prepared with emulsified perfluoroalkanes as blowing agents. J Cell Plast 28(5):486–495. https://doi.org/10.1177/0021955X9202800503
8. Londrigan ME, Snider SC, Trout KG (1993) K-Factor Improvement via Perfluorinated Hydrocarbons. J Cell Plast 29(6):544–555. https://doi.org/10.1177/0021955X9302900603
9. Yu-Hallada LC, McLellan KP, Wierzbicki RJ, Reichel CJ (1993) Improved rigid insulating polyurethane foams prepared with HCFCs and perfluoroalkanes. J Cell Plast 29(6):589–596. https://doi.org/10.1177/0021955X9302900606
10. Volkert O (1995) Cyclopentane-blown rigid foams for refrigerators. J Cell Plast 31(3):210–216. https://doi.org/10.1177/0021955X9503100302
11. Schuetz MA, Glicksman LR (1984) A Basic study of heat transfer through foam insulation. J Cell Plast 20(2):114–121. https://doi.org/10.1177/0021955X8402000203
12. Glicksman L, Schuetz M, Sinofsky M (1987) Radiation heat transfer in foam insulation. Int J Heat Mass Transf 30(1):187–197. https://doi.org/10.1016/0017-9310(87)90071-8
13. Jain AK, Briegleb BP, Minschwaner K, Wuebbles DJ (2000) Radiative forcings and global warming potentials of 39 greenhouse gases. J Geophys Res Atmos 105(D16):20773–20790. https://doi.org/10.1029/2000JD900241
14. Hodnebrog, Etminan M, Fuglestvedt JS, Marston G, Myhre G, Nielsen CJ, Shine KP, Wallington TJ (2013) Global warming potentials and radiative efficiencies of halocarbons and related compounds: a comprehensive review. Rev Geophys 51(2):300–378. https://doi.org/10.1002/rog.20013
15. Mühle J, Ganesan AL, Miller BR, Salameh PK, Harth CM, Greally BR, Rigby M, Porter LW, Steele LP, Trudinger CM, Krummel PB, O'Doherty S, Fraser PJ, Simmonds PG, Prinn RG, Weiss RF (2010) Perfluorocarbons in the global atmosphere: tetrafluoromethane, hexafluoroethane, and octafluoropropane. Atmos Chem Phys 10(11):5145–5164. https://doi.org/10.5194/acp-10-5145-2010
16. Brondi C, Mosciatti T, Di Maio E (2022) Ostwald ripening modulation by organofluorine additives in rigid polyurethane foams.

Ind Eng Chem Res 61(40):14868–14880. https://doi.org/10.1021/acs.iecr.2c01829
17. Hamann M, Andrieux S, Schütte M, Telkemeyer D, Ranft M, Drenckhan W (2023) Directing the pore size of rigid polyurethane foam via controlled air entrainment. J Cell Plast 0(0):1–14. https://doi.org/10.1177/0021955X231152680
18. Klostermann, M.; Schiller, C.; Venzmer, J.; Eilbracht, C. Production of fine cell foams using a cell aging inhibitor. US 2018/0327563 A1, 2018.
19. Kızılersü A, Kreer M, Thomas AW (2018) The Weibull distribution. Significance 15(2):10–11. https://doi.org/10.1111/j.1740-9713.2018.01123.x
20. Magrabi SA, Dlugogorski BZ, Jameson GJ (1999) Bubble size distribution and coarsening of aqueous foams. Chem Eng Sci 54(18):4007–4022. https://doi.org/10.1016/S0009-2509(99)00098-6
21. Stevenson P, Sederman AJ, Mantle MD, Li X, Gladden LF (2010) Measurement of bubble size distribution in a gas-liquid foam using pulsed-field gradient nuclear magnetic resonance. J Colloid Interface Sci 352(1):114–120. https://doi.org/10.1016/j.jcis.2010.08.018
22. Schümann M, Günther S, Odenbach S (2014) The effect of magnetic particles on pore size distribution in soft polyurethane foams. Smart Mater Struct 23(7). https://doi.org/10.1088/0964-1726/23/7/075011
23. Kong M, Bhattacharya RN, James C, Basu A (2005) A statistical approach to estimate the 3D size distribution of spheres from 2D size distributions. GSA Bull 117(1–2):244–249. https://doi.org/10.1130/B25000.1
24. Pinto J, Solórzano E, Rodriguez-Perez MA, De Saja JA (2013) Characterization of the cellular structure based on user-interactive image analysis procedures. J Cell Plast 49(6):555–575. https://doi.org/10.1177/0021955X13503847
25. Peyrton J, Avérous L (2021) Structure-properties relationships of cellular materials from biobased polyurethane foams. Mater Sci Eng R Reports 145:100608. https://doi.org/10.1016/j.mser.2021.100608
26. Bisperink CGJ, Ronteltap AD, Prins A (1992) Bubble-size distributions in foams. Adv Colloid Interface Sci 38(C):13–32. https://doi.org/10.1016/0001-8686(92)80040-5
27. Bhakta A, Ruckenstein E (1997) Decay of standing foams: drainage, coalescence and collapse. Adv Colloid Interface Sci 70(1–3):1–124. https://doi.org/10.1016/s0001-8686(97)00031-6
28. Cantat I, Cohen-Added S, Elias F, Graner F, Höhler R, Pitois O, Rouyer F, Saint-Jalmes A (2013) Foams Structure and Dynamics, 1st edn. Oxford University Press, Oxford
29. Langevin D (2021) Emulsions, Microemulsions and Foams; Springer Nature. https://doi.org/10.1007/978-3-030-55681-5
30. Weaire D, Hutzler S (1999) The Physics of Foams. Oxford University Press, Oxford
31. Boos J, Drenckhan W, Stubenrauch C (2013) Protocol for studying aqueous foams stabilized by surfactant mixtures. J Surfactants Deterg 16(1):1–12. https://doi.org/10.1007/s11743-012-1416-2
32. Denkov ND (2004) Mechanisms of foam destruction by oil-based antifoams. Langmuir 20(22):9463–9505. https://doi.org/10.1021/la049676o
33. De Icaza M, Jiménez-Ceniceros A, Castaño VM (1994) Statistical distribution functions in 2D foams. J Appl Phys 76(11):7317–7321. https://doi.org/10.1063/1.358020
34. Thomas GL, de Almeida RMC, Graner F (2006) Coarsening of three-dimensional grains in crystals, or bubbles in dry foams, tends towards a universal, statistically scale-invariant regime. Phys Rev E 74(2):21–24. https://doi.org/10.1103/physreve.74.021407
35. Weaire D, Pageron V (1990) Frustrated froth: evolution of foam inhibited by an insoluble gaseous component. Philos Mag Lett 62(6):417–421. https://doi.org/10.1080/09500839008215544
36. Rio E, Drenckhan W, Salonen A, Langevin D (2014) Unusually stable liquid foams. Adv Colloid Interface Sci 205:74–86. https://doi.org/10.1016/j.cis.2013.10.023